Toward Real-Time Microearthquake Event Detection and Location in Anisotropic Media Using a Multiscale Approach for EGS Collab Experiments

Yu Chen[1], Lianjie Huang[1], Jonathan Ajo-Franklin[2], Timothy J. Kneafsey[2], and EGS Collab Team[*]

[1]Los Alamos National Laboratory, Los Alamos, NM 87545, USA

[2]Lawrence Berkeley National Laboratory, Berkeley, CA 94720, USA

Keywords

Anisotropic media, correlation coefficient, detection, Enhanced Geothermal Systems, EGS stimulation, location, MEQ, MEQ, multiscale, real-time

ABSTRACT

Real-time, automatic microearthquake detection and location provides crucial information on fracture growth during stimulation and is planned for the second phase of the EGS Collab stimulation experiments. We study the feasibility of real-time detection and location of microearthquake events for the sensor distribution in the EGS Collab Experiment I, using eighteen 3C accelerometers. We pre-compute a microearthquake waveform database for a 43 x 43 x 43 grid with a grid interval of 1 m using an anisotropic elastic-wave modeling tool. We then compute correlation coefficients between recorded seismograms and those in the waveform database using a moving time window and search for the highest correction coefficients to detect

---

[*] J. Ajo-Franklin, S.J. Bauer, T. Baumgartner, K. Beckers, D. Blankenship, A. Bonneville, L. Boyd, S.T. Brown, J.A. Burghardt, T. Chen, Y. Chen, K. Condon, P.J. Cook, P.F. Dobson, T. Doe, C.A. Doughty, D. Elsworth, J. Feldman, A. Foris, L.P. Frash, Z. Frone, P. Fu, K. Gao, A. Ghassemi, H. Gudmundsdottir, Y. Guglielmi, G. Guthrie, B. Haimson, A. Hawkins, J. Heise, M. Horn, R.N. Horne, J. Horner, M. Hu, H. Huang, L. Huang, K. Im, M. Ingraham, T.C. Johnson, B. Johnston, S. Karra, K. Kim, D.K. King, T. Kneafsey, H. Knox, J. Knox, D. Kumar, K. Kutun, M. Lee, K. Li, R. Lopez, M. Maceira, N. Makedonska, C. Marone, E. Mattson, M.W. McClure, J. McLennan, T. McLing, R.J. Mellors, E. Metcalfe, J. Miskimins, J.P. Morris, S. Nakagawa, G. Neupane, G. Newman, A. Nieto, C.M. Oldenburg, W. Pan, R. Pawar, P. Petrov, B. Pietzyk, R. Podgorney, Y. Polsky, J. Popejoy S. Porse, S. Richard, B.Q. Roberts, M. Robertson, W. Roggenthen, J. Rutqvist, D. Rynders, H. Santos-Villalobos, M. Schoenball, P. Schwering, V. Sesetty, A. Singh, M.M. Smith, H. Sone, F.A. Soom, C.E. Strickland, J. Su, J.N. Thomle, C. Ulrich, N. Uzunlar, A. Vachaparampil, C.A. Valladao, W. Vandermeer, G. Vandine, D. Vardiman, V.R. Vermeul, J.L. Wagoner, H.F. Wang, J. Weers, J. White, M.D. White, P. Winterfeld, T. Wood, H. Wu, Y.S. Wu, Y. Wu, E.C. Yildirim, Y. Zhang, Y.Q. Zhang, J. Zhou, Q. Zhou, M.D. Zoback

and locate microearthquake events simultaneously. Toward real-time monitoring, we employ a multiscale event scanning method that requires only 0.03% of the computation cost of the global search for 43 x 43 x 43 grid points and every scanning time step, making real-time detection and location feasible. We verify the feasibility of our multiscale microearthquake event detection and location for real-time monitoring using noise-free and noisy synthetic microearthquake data for the sensor distribution in the EGS Collab Experiment I.

1. Introduction

Under the EGS Collab project supported by the U.S. Department of Energy's Geothermal Technologies Office (GTO), U.S. national laboratories and universities are conducting intermediate (on the order of 10 m)-scale field experiments to refine our understanding of rock mass response to stimulation and provide a test bed for the validation of thermal hydrological-mechanical-chemical (THMC) modeling approaches as well as novel monitoring tools (Dobson et al., 2017; Kneafsey et al., 2018).

Real-time microearthquake (MEQ) monitoring is currently the most efficient approach to obtaining a spatio-temporal image of fracture growth during stimulation. Real-time monitoring is a standard operational procedure for a traffic-light stimulation system attempting to control injection and mitigate risk of induced earthquakes (Maxwell, 2014). During stimulation experiments, it is important to identify the direction and extension of fracture growth, and understand the relationship between injection rates and fracture growth during stimulation. EGS stimulation could also trigger geohazards on pre-existing faults or cause a rupture in an unexpected direction, which requires real-time monitoring.

Various MEQ detection and location methods have been developed for real-time monitoring. We classify previous studies into three categories. The first category of the methods detects seismic phases and invert arrival-times of those seismic phases (e.g. Khadhraoui et al., 2010). These methods are the least time consuming. However, it is difficult to distinguish seismic phases, particularly for MEQ in anisotropic media that can cause shear-wave splitting. Detecting the arrival times is even more challenging for MEQ in anisotropic media. The second category of the methods is based on cross-correlation of MEQ waveforms between recorded and template data/pre-computed waveforms (e.g. Zhang and Zhang, 2016). The methods based on cross-correlation usually cannot detect multiple events occurring at the same time. There are several peak values in the cross-correlation of the waveforms that have multiple events. It is challenging to distinguish possible combination of those phases. The third category of the methods migrates seismic energy back to the best hypocenter location (e.g., Nakata and Beroza, 2016). These methods have potential to search several events occurred at the same time. However, it is difficult to distinguish seismic phases used in these methods. Most of previous studies concentrated on MEQ event detection in isotropic media. Real-time seismic phase identification and event detection/location for MEQ events in anisotropic media are more challenging than those in isotropic media.

We develop a new approach to real-time detection and location of MEQ events in anisotropic media. Our method is based on a computationally efficient multiscale event detection and

location method. First, we use an elastic-wave modeling tool for anisotropic media to pre-compute an MEQ waveform database for a 43 x 43 x 43 grid model with a grid interval of 1 m. We then scan the largest correlation coefficients among moving time windows between the recorded seismograms and the waveform database seismograms to detect and locate MEQ events simultaneously. Our method can identify multiple events that occur at a same/similar time, with overlapping waveforms. We verify our new method using synthetic MEQ waveforms for the sensor distribution in the EGS Collab Experiment I, and demonstrate that our method can efficiently detect and locate the synthetic MEQ events in nearly real time.

2. Methodology

2.1 MEQ event detection

We employ a short-time-average/long-time-average (STA/LTA) method for MEQ event detection. The STA/LTA method uses usually either the L_1- or L_2-norm. In this study, we adopt the L_2-norm to compute the energy ratio between an STA short time window and an LTA long time window preceding the computed time sample. The ratio of an STA value to an LTA value is greater than one for an MEQ event. We select the STA/LTA threshold of two for real-time monitoring of significant MEQ events. The STA/LTA method significantly improves detection of weak MEQ events in noisy data compared with traditional amplitude threshold triggering algorithms. In addition, the STA/LTA method can maintain a consistent signal-to-noise ratio (SNR) for varying noise levels, but the amplitude threshold triggering algorithm must change the triggering threshold for different noise levels.

2.2 MEQ waveform database pre-computed using anisotropic elastic-wave modeling

We pre-compute the MEQ waveforms using an anisotropic finite-difference waveform modeling method (Gao and Huang, 2017) in heterogeneous and anisotropic media. For vertical transverse isotropic (VTI) media, we set the P-wave velocities along the fast and slow axes as 6.5 km/s and 4.8 km/s, respectively, the S-wave velocities along the fast and slow axes as 4.3 km/s and 3.3 km/s, respectively, and the density as 2.85 x 10^3 kg/m^3 (Chen et al., 2018). We compute the stiffness matrix C_{ij} in the VTI medium as follow:

$$C = \begin{bmatrix} 120.4125 & 58.3395 & -29.1698 & 0 & 0 & 0 \\ & 120.4125 & -29.1698 & 0 & 0 & 0 \\ & & 65.664 & 0 & 0 & 0 \\ & & & 52.6965 & 0 & 0 \\ & & & & 52.6965 & 0 \\ & & & & & 31.0365 \end{bmatrix}.$$

We then compute the MEQ waveforms based on the stiffness model.

We apply envelope transformation to both the computed synthetic waveforms and the recorded waveforms. The envelope transformation is capable of reversing negative polarity to positive polarity. Varying polarities of different phases decrease the correlation coefficients. The complex waveforms with multiple wiggles would generate local minima, and the waveforms with

different frequencies would generate a low correlation coefficient. Therefore, we use the envelope transformation to avoid the cycle-skipping effect. We normalize the envelopes to balance the amplitudes between P, SV and SH phases. Envelop normalization can avoid obtaining a correlation coefficient dominated by specific strong-amplitude phases.

2.3 Multiscale MEQ event scanning

We develop a multiscale event scanning algorithm to grid-search the best occurring time and hypocenter location using the highest correlation coefficients between full-waveform envelopes of the recorded data and the synthetics. When the STA/LTA value is greater than a given threshold, our event-scanning algorithm searches the 43 x 43 x 43 grids and all time steps within a time window. We determine an MEQ event when its correlation coefficient is higher than a threshold value. We identify multiple MEQ events that occur at the same/similar time when several similar correlation coefficients are greater the threshold value.

Toward real-time monitoring, we employ a computationally efficient multiscale method for MEQ event detection and location in 3D space. We schematically illustrate the multiscale method in 2D in Figure 1. To determine the grid points with the largest correlation coefficients, we first compute correlation coefficients of waveforms within a 7 x7 x 7 grid (Scale 1 grid on the left panel of Figure 1). The grid interval is 6 m. The time step for moving time windows to calculate correlation coefficients is 20 time sample intervals of MEQ waveforms. After scanning Scale 1 grids (the left panel in Figure 1) and obtaining a grid point with one of the highest correlation coefficients, we continue to scan within a 7 x7 x 7 grid (Scale 2 grid on the right panel of Figure 1) with a grid interval of 1 m centered on the inverted grid point on the Scale 1 grid, and determine a grid point with the largest correlation coefficient of waveforms. During the scanning process in Scale 2, the time step for the moving windows to calculate the correlation coefficients is one sample interval of MEQ waveforms. We can continue to scan grid points within a finer grid, till achieving the spatial resolution needed for real-time monitoring. Such a multiscale event detection and location method requires 24010 computations if the moving time window contains 1000 waveform samples. The computation cost required for the method is only 0.03% of that required for the global search within 43 x 43 x 43 grid points with a grid interval of 1 m and a moving window of 1000 waveform samples. The vast decrease in computational cost of our multiscale scanning method makes real-time MEQ detection and location feasible.

3. Numerical examples

The EGS Collab project has initiated a field experiment at the Sanford Underground Research Facility (SURF) site located at the former site of the Homestake Gold Mine in Lead, South Dakota. The experiment is located within a drift, approximately 1.5 km beneath the surface. An injection well (green cylinder in Figure 2) and a production well (red cylinder in Figure 2) have been drilled to create multiple fractures (blue circles in Figure 2) with the diameters of approximately 10 m. In addition, six monitoring wells have been drilled for the experiment (yellow cylinders in Figure 2). Four of these wells (PST, PSB, PDT and PBT in Figure 2) are parallel to the potential fractures, and two wells (OT, OB in Figure 2) are orthogonal to the created fractures. Eighteen geophones, illustrated by black spheres in Figure 2, are deployed within the monitoring wells.

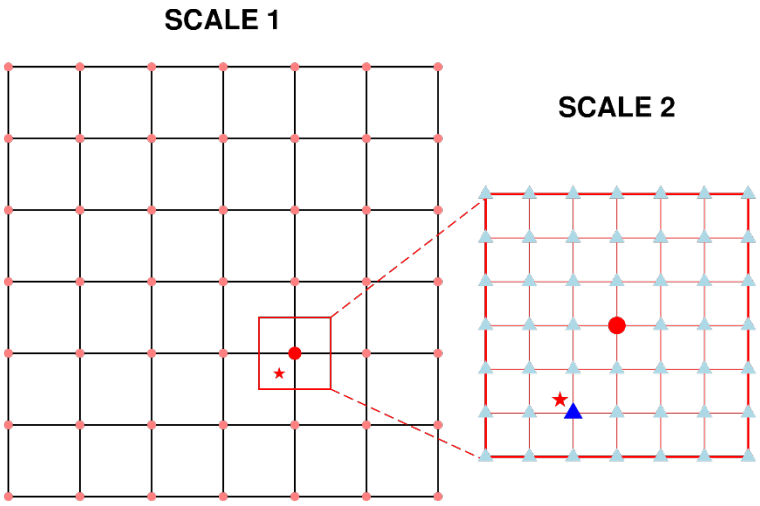

Figure 1: Schematic illustration of our multiscale MEQ event scanning method. Left panel: The heavy red dot represents the inverted MEQ event location in Scale 1 for the true MEQ event labeled as the red star. The red box is the scanning region for Scale 2 with a finer grid. It is centered on the red dot. Right panel: A finer grid (Scale 2) within the red box on the Left panel. The blue triangle represents the inverted MEQ location in Scale 2.

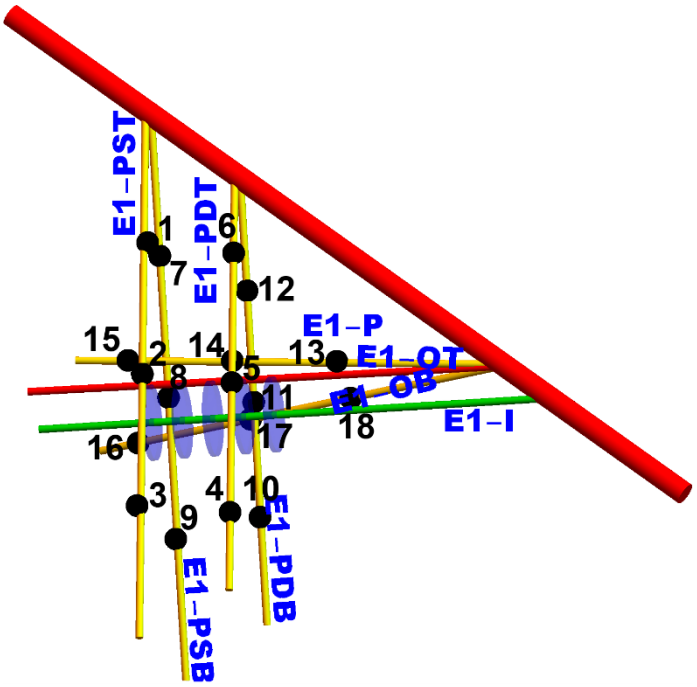

Figure 2: Schematic illustration of the monitoring wells at SURF for the EGS Collab Experiment 1. The monitoring wells drilled from the drift (red cylinder) are in yellow. The injection well is in green, and the production well is in red. The circular regions in blue are the fractures to be created by EGS stimulations. The geophones (black spheres labelled by black numbers) are distributed within the monitoring wells in yellow to monitor induced MEQs evenly distributed within the created fractures in the blue circular regions.

We verify our multiscale scanning method for real-time MEQ monitoring using both noise-free and noisy synthetic MEQ data for the EGS Collab Experiment I. We generate 110 MEQ events at random locations within a 43 x 43 x 43 m cube (black spheres in Figure 3). The MEQ events include 90 single events, 8 pairs of doublet events, and 1 group of triplet events. In EGS Collab Experiment I (Figure 2), induced MEQ events should occur in the center region within/around the fractures. These geophones have a good azimuthal coverage for MEQ event location. Because EGS fracturing may trigger MEQ events, we also generate some MEQ events outside the fracture zones. We compute synthetic waveforms with a length of 60 seconds consisting of all MEQ events with a strike-slip focal mechanism using our anisotropic finite-difference waveform modeling method.

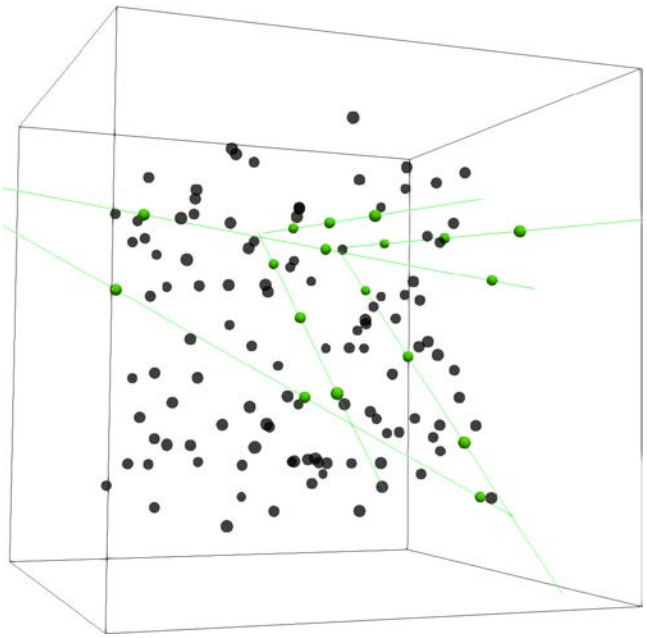

Figure 3: Spatial locations of 110 synthetic MEQ events (black spheres) for the EGS Collab Experiment I. Green lines represents the monitoring wells. The geophones (green spheres) are distributed within the monitoring wells.

In the first numerical test, we apply our multiscale scanning method for event detection and location to noise-free synthetic MEQ data. Our method detects and locates 113 MEQ events, including all of the 110 synthetic events and 3 false events (Figure 4). The result verifies that our method is capable of detecting and locating doublets and a triplet simultaneously, in addition to the single events. The standard deviation error of event locations for the 110 true events is 1.5 m. In Figure 4, we plot the true (black spheres) and located (red spheres) MEQ events with radii of 0.5 m. The MEQ events within the center region surrounded by the monitoring wells are well located, as shown by the partially/fully overlapped red and black spheres. For the events with a good azimuthal coverage, the standard deviation location error is approximately 0.5 m. For the events outside the center region surrounded by the monitoring wells, the standard deviation location error is 2.7 m.

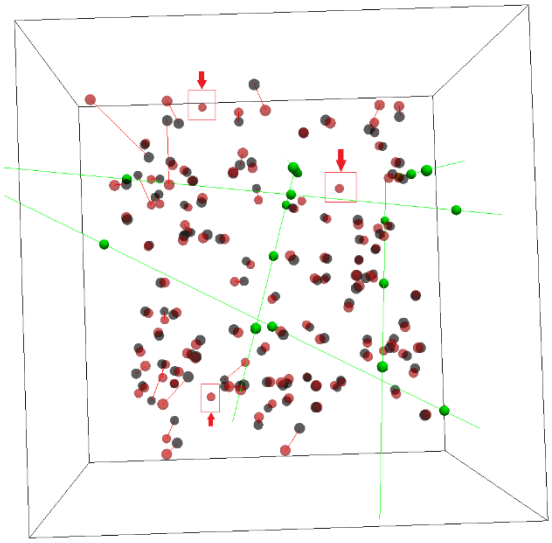

Figure 4: The synthetic (black spheres) MEQ events and the located (red spheres) MEQ events obtained using our multiscale scanning method with noise-free MEQ data. Green lines represent monitoring wells at SURF for the EGS Collab Experiment I. The geophones (green spheres) are distributed within the monitoring wells. Lengths of red lines connecting the synthetic (black) and the located (red) events represent the location errors. Red rectangles and arrows highlight the three false events.

We display three examples of waveform envelope fitting for a single event (top panel in Figure 5), a pair of doublet events (middle panel in Figure 5) and a group of triplet events (bottom panel in Figure 5). We refer to two MEQ events occurred at the same time as the doublet events, and three MEQ events occurred at the same time as the triplet events. In the top panel, the MEQ event has a hypocenter location (X, Y, Z) at (15.8 m, 26.4 m, 27.9 m). The event location obtained using our multiscale scanning method is (16 m, 26 m, 28 m). The synthetic waveform envelopes (blue traces) match well with the data envelopes (black traces), with a correlation coefficient of 0.97. In the middle panel, the two events are located at (26.1 m, 18.8 m, 22.3 m) and (26.1 m, 18.8 m, 4.8 m). The locations of the two events obtained using our multiscale scanning method are at (26 m, 18 m, 22 m) and (26 m, 19 m, 4 m), respectively. Blue traces represent synthetic envelopes for the two events, and they fit the data waveforms well (black traces). In bottom panel, the triplet events' hypocenter locations are at (29.1 m, 34.2 m, 30.1 m), (35.3 m, 9.7 m, 25.2 m), and (5.2 m, 20.2 m, 5.4 m). The locations obtained using our multiscale scanning method are (29 m, 34 m, 30 m), (35 m, 10 m, 26 m), and (6 m, 21 m, 6 m), respectively. The waveform envelope fittings indicate that our multiscale scanning method can fit the recorded waveforms and obtain the adjacent grid points to the true event locations.

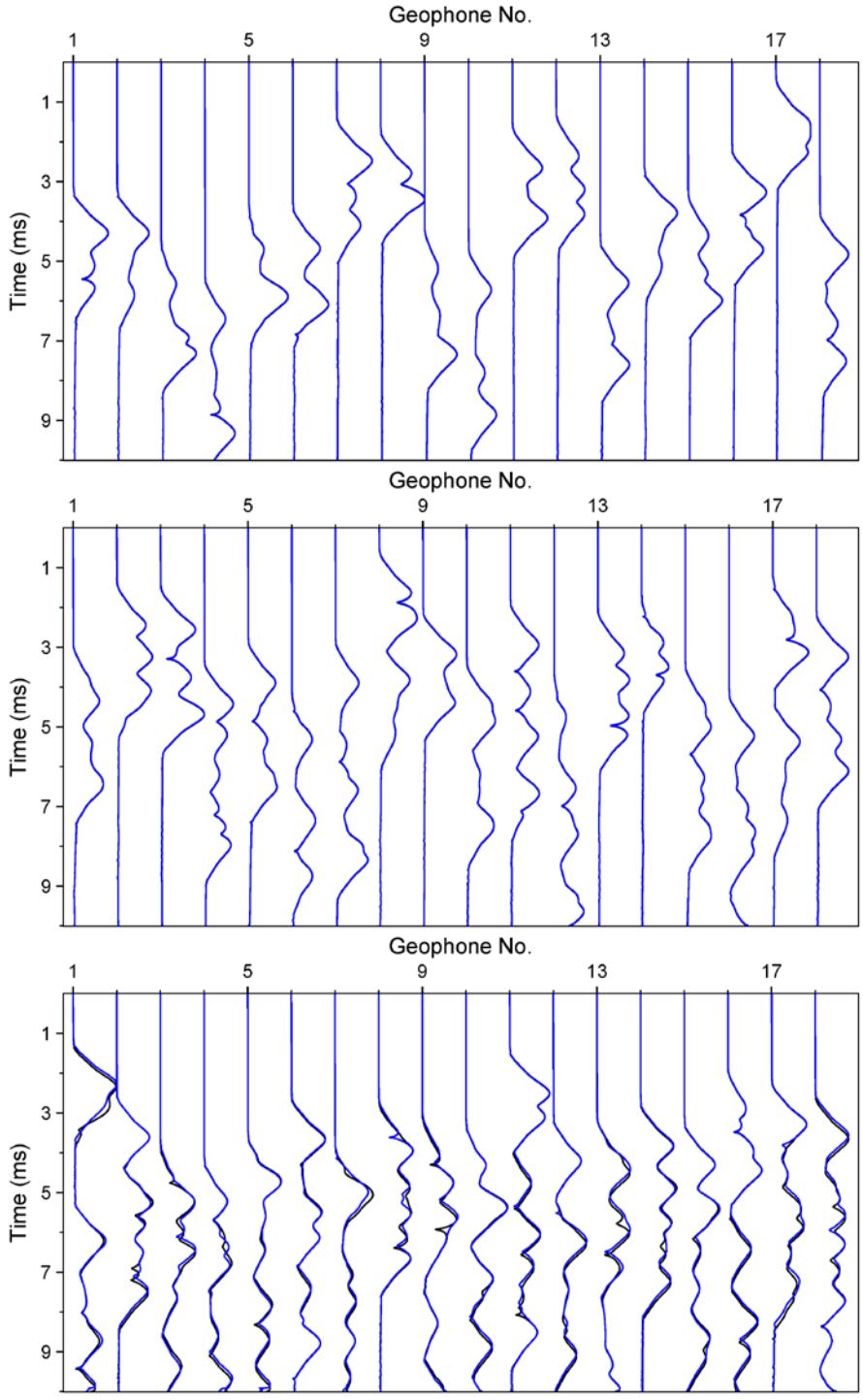

Figure 5: Examples of MEQ waveform envelope fitting for a single MEQ event (top panel), doublet events (middle panel), and triplet events (bottom panel) for noise-free data. Black traces in the panels represent the waveform envelopes of the true MEQ event, and blue traces represent the waveform envelopes of the located MEQ events. The geophone numbers in this figure corresponds to those in Figure 1.

In the second numerical test, we add truncated real seismic noise, with amplitudes normalized to 10% of the synthetic MEQ data with the maximum amplitude among all waveforms in the previous numerical test. Because we generate all MEQ waveforms using a strike-slip focal mechanism and those events are in different distances from the receivers, the waveform amplitudes recorded by different geophones vary greatly. Some of these waveforms with added noise become very noisy.

Before applying our multiscale scanning method, we use the STA/LTA method to detect the events. The STA/LTA algorithm can detect signals from noisy data. We employ 50 time samples (approximately a period of the data) for the STA window and 1000 time samples for the LTA window. We show an example of the noisy waveforms (black traces) from a receiver far away from an event and their stacked STA/LTA trace (red trace) in Figure 6. The P and S waveforms (black traces) do not exhibit clear P and S onsets, and it is difficult for the traditional method based on an amplitude threshold to detect the P and S arrivals. By contrast, the STA/LTA method can provide clear onsets for the P and/or S arrivals, indicating there exists an MEQ event.

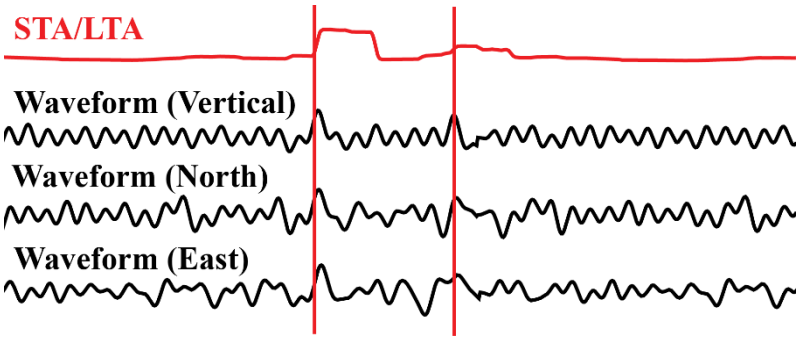

Figure 6: The STA/LTA method can clearly detect the onsets of P and/or S arrivals of an MEQ event for noisy data. Black traces are noisy synthetic MEQ waveforms in vertical, north and east directions. The red trace is the stacked STA/LTA traces of the three component MEQ waveforms.

Once the STA/LTA detects an event onset, we select a searching window of data and begin searching the event occurring times and hypocenter locations using our multiscale scanning method. The method detects 104 of the 110 MEQ events, and generates 8 false events. We display the result in Figure 7. We study the hypocenter locations of those events, and find that the six undetected/unlocated events highlighted by black rectangles in Figure 7 are located outside of the center region. Therefore, those events have very low SNRs and cannot be detected using our method.

The standard deviation error of event locations for the 104 events is 2.0 m, a little larger than that for the noise-free data. The MEQ events within the center region are well located. The standard deviation location error for those events is approximately 0.5 m, similar to the result for the noise-free data. For the events outside the center region, the standard deviation location error is 4.4 m. The low signal-to-noise ratio could lead to a large uncertainty.

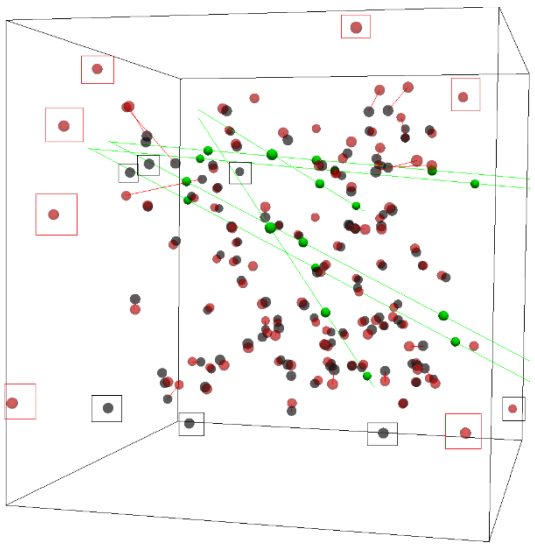

Figure 7: The synthetic (black spheres) MEQ events and the located (red spheres) MEQ events obtained using our multiscale scanning method with noisy MEQ data. Green lines represent monitoring wells at SURF for the EGS Collab Experiment I. The geophones (green spheres) are distributed within the monitoring wells. Lengths of red lines connecting the synthetic (black) and the located (red) events represent the location errors. Red rectangles highlight the false events. Black rectangles highlight the undetected events.

We show three examples of waveform envelope fitting for the same events as those in the previous numerical test. Those events include a single event (top panel in Figure 8), doublet events (middle panel in Figure 8) and triplet events (bottom panel in Figure 8). In the top panel, the MEQ event has a hypocenter location at (15.8 m, 26.4 m, 27.9 m). The located event is at (16 m, 26 m, 28 m). In the middle panel, there are two events occurred at the same time with the locations at (26.1 m, 18.8 m, 22.3 m) and (26.1 m, 18.8 m, 4.8 m). The located events are at (26 m, 19 m, 22 m) and (26 m, 19 m, 5 m), respectively. In the bottom panel, the true triplet events have hypocenter locations at (29.1 m, 34.2 m, 30.1 m), (35.3 m, 9.7 m, 25.2 m), and (5.2 m, 20.2 m, 5.4 m). The located triplet events are at (29 m, 34 m, 29 m), (35 m, 10 m, 26 m), and (5 m, 20 m, 5 m), respectively. The waveform envelope fittings indicate that our multiscale scanning method can fit the recorded waveforms for noisy data and obtain the adjacent grid points to the true event locations.

We measure the computation cost of our multiscale scanning method to evaluate its capability for real-time monitoring. We run our method on a desktop workstation and use openMP to accelerate the computation. We assess the parallel-computing performance for a desktop computer with a 2.3 GHz Xeon processor. Our program includes three parts, including database input, STA/LTA detection and MEQ event scanning. Because the database is pre-computed and we need to read in the database once only, the consumed wall-clock time can be ignored for real-time monitoring. The STA/LTA computation of the 60-s waveforms with a sample interval of 10^{-5} s takes 5 s only. The most time-consuming part is event scanning. For event scanning, we use openMP to parallelize the correlation coefficient computation for the 18 geophones. Eighteen threads should be the best for the parallel computation. For the 110 MEQ events in our numerical tests, we plot the average computational time per MEQ event as a function of the number of

threads in Figure 9. The average computation time per MEQ event is approximately 8 s when using one thread, 1.4 s when using nine threads, and 1 s when using 18 threads. Therefore, our multiscale scanning method is capable of detecting and locating MEQ events in nearly real time.

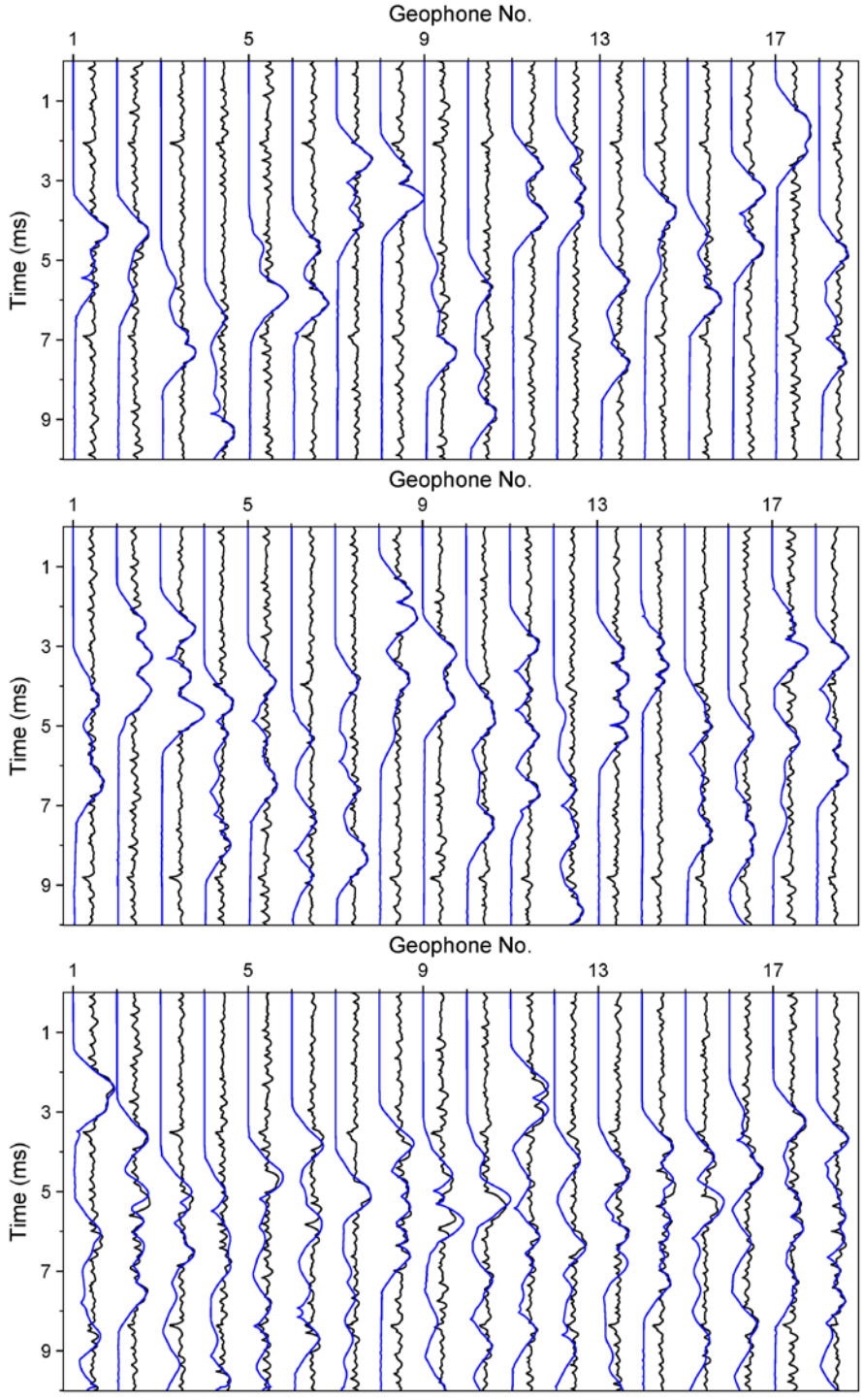

Figure 8: Examples of MEQ waveform envelope fitting for a single MEQ event (top panel), doublet events (middle panel), and triplet events (bottom panel) for noisy data. Black traces in the panels represent the waveform envelopes of the true MEQ event, and blue traces represent the waveform envelopes of the located MEQ events. The geophone numbers in this figure corresponds to those in Figure 1.

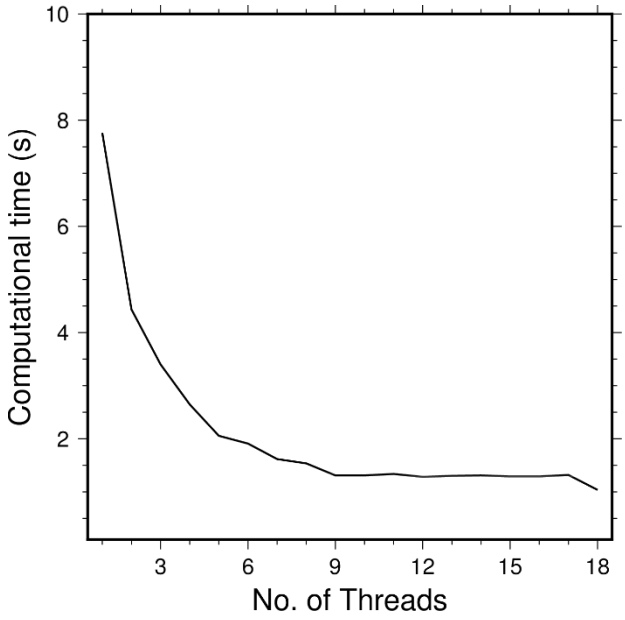

Figure 9: Average computational time per event for our multiscale event scanning algorithm versus the number of threads of a desktop computer with a 2.3 GHz Xeon processor.

4. Conclusions

We have developed a multiscale scanning method toward real time microearthquake monitoring during EGS stimulation. Our new method searches for the event occurring time and hypocenter location using highest correlation coefficients between recorded seismograms and a pre-computed waveform database. The method employs a multiscale event scanning method to greatly reduce the computation cost of the global search for 43x43x43 grid points. We verify the feasibility of our multiscale MEQ event detection and location method for real-time monitoring using noise-free and noisy synthetic data for the sensor distribution in the EGS Collab Experiment I. We generate synthetic waveforms for 110 MEQ events with/without real seismic noise. Our method is capable of detecting and locating all 110 MEQ events using noise-free data and 104 MEQ events using noisy data. Most importantly, our method can detect multiple events occurred at the same time. Our method takes approximately one second to detect and locate one MEQ event on a desktop computer with a 2.3 GHz Xeon processor, and has great potential for real-time MEQ monitoring during EGS stimulation.

ACKNOWLEDGMENTS

This material was based upon work supported by the U.S. Department of Energy, Office of Energy Efficiency and Renewable Energy (EERE), Office of Technology Development, Geothermal Technologies Office, under Award Number DE-AC52-06NA25396 to Los Alamos National Laboratory (LANL). The United States Government retains, and the publisher, by accepting the article for publication, acknowledges that the United States Government retains a non-exclusive, paid-up, irrevocable, world-wide license to publish or reproduce the published

form of this manuscript, or allow others to do so, for United States Government purposes. The computation was performed using super-computers of LANL's Institutional Computing Program.

REFERENCES

Chen, Y., Huang, L., and EGS Collab Team "Microearthquake Hypocenter-Location and Focal-Mechanism Inversions for the EGS Collab Project: A Synthetic Study." Proceedings: 43rd Workshop on Geothermal Reservoir Engineering, Stanford University, Stanford, CA (2018).

Dobson, P., Kneafsey, T.J., Blankenship, D., Valladao, C., Morris, J., Knox, H., Schwering, P., White, M., Doe, T., Roggenthen, W., Mattson, E., Podgorney, R., Johnson, T., Ajo-Franklin, J., and EGS Collab Team, "An Introduction to the EGS Collab SIGMA-V Project: Stimulation Investigations for Geothermal Modeling Analysis and Validation," GRC Transactions, 41, (2017), 837-849.

Gao, K., and Huang, L., "An improved rotated staggered-grid finite-difference method with fourth-order temporal accuracy for elastic-wave modeling in anisotropic media." Journal of Computational Physics, 350, (2017), 361-386.

Huang, L., Chen, Y., Gao, K., Fu, P., Morris, J., Ajo-Franklin, J., Nakagawa, S., and EGS Collab Team, "Numerical modeling of seismic and displacement-based monitoring for the EGS Collab Project." GRC Transaction, 41, (2017), 893-909.

Khadhraoui, B., Leslie, D., Drew, J., and Jones, R., "Real-time detection and localization of microseismic events", SEG Expanded Abstract, Denver, CO (2010).

Kneafsey, T.J., Dobson, P., Blankenship, D., Morris, J., Knox, H., Schwering, P., White, M., Doe, T., Roggenthen, W., Mattson, E., Podgorney, R., Johnson, T., Ajo-Franklin, J., Valladao, C., and the EGS Collab team "An Overview of the EGS Collab Project: Field Validation of Coupled Process Modeling of Fracturing and Fluid Flow at the Sanford Underground Research Facility, Lead, SD." Proceedings: 43rd Workshop on Geothermal Reservoir Engineering, Stanford University, Stanford, CA (2018).

Maxwell, S. "Microseismic Imaging of Hydraulic Fracturing." Society of Exploration Geophysicists (2014).

Nakata, N., and Beroza, G., "Reverse time migration for microseismic sources using the geometric mean as an imaging condition" Geophysics, 81, (2016), 251-259.

Zhang, X., and Zhang, J., "Microseismic search engine for real-time estimation of source location and focal mechanism" Geophysics, 81, (2016), 169-181.